ENVIRONMENTAL RESEARCH
LETTERS

CrossMark

OPEN ACCESS

LETTER

Modeling evidence for large, ENSO-driven interannual wintertime AMOC variability

K L Smith[1,3,*] ⬥ and L M Polvani[2,3] ⬥

[1] Department of Physical and Environmental Sciences, University of Toronto Scarborough, Toronto, ON, Canada
[2] Department of Applied Physics and Mathematics, Department of Earth and Environmental Sciences, Columbia University, New York, NY, United States of America
[3] Division of Ocean and Climate Physics, Lamont-Doherty Earth Observatory, Palisades, NY, United States of America
[*] Author to whom any correspondence should be addressed.

E-mail: karen.smith@utoronto.ca

Abstract
Recently established North Atlantic ocean observing arrays, such as RAPID/MOCHA, have revealed a large degree of high-frequency variability in the Atlantic Meridional Overturning Circulation (AMOC). Climate modeling studies of the AMOC, however, have traditionally focused on the low-frequency variability of the annual mean AMOC, with an emphasis on multi-decadal and longer time-scale variability. Thus, little is known about the sources of interannual wintertime, wind-driven AMOC variability. Analyzing the Community Earth System Model, we here show the existence of a robust leading mode of interannual variability in the wintertime AMOC that is distinct from the leading mode of the annual mean. We further show that this mode of variability is significantly linked to the El Niño-Southern Oscillation via the North Atlantic Oscillation.

1. Introduction

Over the past decade, moored observational arrays stretching across the Atlantic Ocean, such as RAPID/MOCHA, OSNAP and MOVE (Frajka-Williams *et al* 2019), have been monitoring the Atlantic Meridional Overturning Circulation (AMOC) at high temporal resolution (Cunningham *et al* 2007, Kanzow *et al* 2010, Smeed *et al* 2014). These unprecedented data sets have revealed a large seasonal cycle and significant high-frequency variability in the AMOC, previously unobserved due to temporal and spatial sparsity of measurements (Cunningham *et al* 2007, Kanzow *et al* 2010). Here, high-frequency AMOC variability refers to variability on intra-annual to interannual time scales.

While observations of the AMOC have been limited until recently, exploration of the AMOC with general circulation models (GCMs) has been an active area of research. The majority of GCM studies have tended to focus on low-frequency AMOC variability, and its role in driving decadal-to-centennial timescale climate variability (e.g. Knight *et al* 2005, Zhang *et al* 2007, Danabasoglu 2008, Danabasoglu *et al* 2012, Delworth *et al* 2017), and thus limited their analysis

to the *annual mean* (or low-pass filtered) AMOC. Nonetheless, high-frequency variability of the AMOC in models has also been investigated (Buckley and Marshall 2016, and references therein): it has been largely attributed to local wind forcing and this has informed the conclusion that the observed high-frequency variability (e.g. in the RAPID time series) is likewise driven by local wind forcing, particularly that associated with the North Atlantic Oscillation (NAO) (Roberts *et al* 2013, Zhao and Johns 2014, Elipot *et al* 2017). Questions remain, however, as to the sources of the NAO variability, and whether such sources can be linked directly to the seasonal AMOC variability.

The aim of this study is to examine the extent to which remote sources of variability, specifically the El Niño-Southern Oscillation (ENSO), can influence the wind-driven, high-frequency AMOC circulation via atmospheric teleconnections and how this influence can be highly seasonal. Improving our understanding of seasonal AMOC variability will aide in our interpretation of ongoing observational programs (Frajka-Williams *et al* 2019), and, thus, advance our ability to detect changes in the AMOC and predict how the AMOC will evolve in response to increasing greenhouse gases.

Here, analyzing two configurations of the Community Earth System Model (CESM), we find robust Ekman-induced variability in the *wintertime* AMOC in the North Atlantic that is significantly linked to ENSO via surface wind-stress anomalies associated with the NAO. We further show that this pattern of variability projects strongly onto the leading mode of the wintertime AMOC, and is distinct from the leading mode of the annual mean AMOC.

2. Methods

2.1. Global climate models

For this study, we employ the CESM (CESM1; Hurrell *et al* 2013). We use both the CAM5 and WACCM4 atmospheric configurations of CESM1, namely CESM1(CAM5) and CESM1(WACCM4), in order to establish the robustness of our results. The atmospheric components of the two configurations differ in the number of vertical levels, horizontal resolution and in their physics parameterizations. In fact, the physics parameterizations are substantially different between the two atmospheric components (Neale *et al* 2010). CESM1(WACCM4) has 66 vertical levels with a model top at 140 km, a horizontal resolution of $1.9° \times 2.5°$, employs the CAM4 atmospheric physics parameterizations and also has specialized parameterizations for gravity waves and interactive middle atmosphere ozone chemistry (Marsh *et al* 2013). CESM1(CAM5) has 26 vertical levels, a horizontal resolution of $0.9° \times 1.25°$ and employs the CAM5 atmospheric physics parameterizations (Hurrell *et al* 2013). Note that the version of CESM1(CAM5) described above is that same version used for the CESM Large Ensemble (LENS) project (Kay *et al* 2015). The CESM1(CAM5) and CESM1(WACCM4) integrations examined here are coupled to identical interactive land, ocean, and sea ice components (Gent *et al* 2011). Notably, the power spectra of ENSO in CESM1(CAM5) and CESM1(WACCM4) are rather different, with that of CESM1(WACCM4) being very similar to the Community Climate System Model version 4 (CCSM4) (pre-industrial ENSO power spectra for CESM1(CAM5) and CCSM4 can be viewed here: http://webext.cgd.ucar.edu/Multi-Case/CVDP_ex/CESM_comparison/nino34.powspec.png). Hereafter, we will refer to CESM1(CAM5) as CAM5 and CESM1(WACCM4) as WACCM4.

2.2. Integrations

The majority of our analysis focuses on the pre-industrial integration of CAM5 that was completed as part of the CESM LENS project (Kay *et al* 2015). We examine 1100 years of this integration, years 401–1500 (we discard the first 400 years to ensure that the ocean is sufficiently equilibrated). We perform similar analysis with a 400 year long integration of WACCM4 with year 2000 forcings. This integration is documented in Smith *et al* (2018).
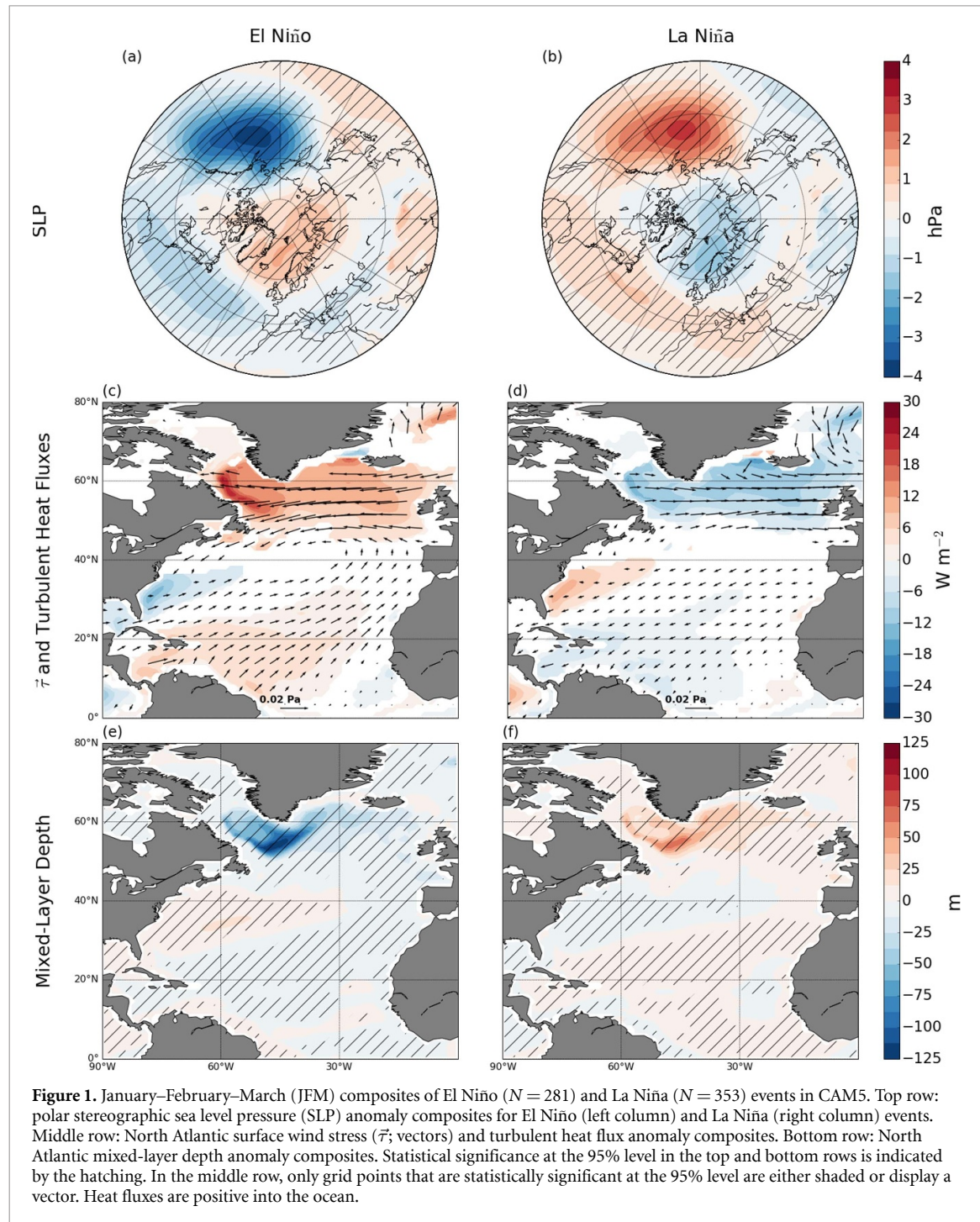
2.3. Analysis

Composite analysis of the AMOC and other variables based on the presence of an El Niño or La Niña event is conducted. ENSO is defined using the 3 month running mean sea surface temperature (SSTs) anomalies averaged over the region 5° S–5° N and 170° W–120° W. An El Niño (La Niña) event is detected when the SST anomalies exceed $+0.5$ °C (-0.5 °C) for at least five consecutive months. Identification of El Niño and La Niña events is based on the National Oceanographic and Atmospheric Administration's Oceanic Niño Index definition (https://origin.cpc.ncep.noaa.gov/products/analysis_monitoring/ensostuff/ONI_v5.php). Using this definition, we find 281 El Niño events and 353 La Niña events in our 1100 year long CAM5 integration, and 117 El Niño events and 128 La Niña events in our 400 year long WACCM4 integration.

We calculate the wintertime (January–February–March (JFM)) NAO index as the leading principal component (PC) time series of sea-level pressure from 20° N–90° N and 90° W–30° E. We also perform PC analysis of the wintertime (JFM) AMOC. The AMOC is defined as the stream function for the zonally-integrated (from west to east, across the Atlantic Basin) meridional volume transport as a function of depth and latitude. By convention, a positive stream function corresponds to a clockwise circulation, with northward transport at the surface and southward transport at depth. Note that no smoothing is applied to any of the model output outside of the tropical SSTs in the definition of ENSO.

3. Results

Before examining the effect of ENSO on the AMOC, we begin by presenting the wintertime (JFM) ENSO-NAO teleconnection in CAM5. While the dynamical connection between ENSO and the NAO remains an area of ongoing research (Mezzina *et al* 2020), several studies have identified a relationship between ENSO and the NAO in winter via the northeastward propagation of planetary waves excited by anomalous convection in the tropical Pacific region (Rodríguez-Fonseca *et al* 2016, and references therein). The teleconnection pathway can be either tropospheric or stratospheric, with El Niño events being associated with the negative phase of the NAO and La Niña events being associated with the positive phase of the NAO (see Polvani *et al* 2017, for example).

Here, using large sample sizes, we find a clear NAO-like sea level pressure (SLP) pattern associated with ENSO. Figures 1(a) and (b) show El Niño and La Niña composites for CAM5 of wintertime SLP anomalies. In the North Pacific region, we clearly see the anomalous low and high pressure teleconnection patterns associated with El Niño and La Niña, respectively. In the North Atlantic region, we

Figure 1. January–February–March (JFM) composites of El Niño ($N = 281$) and La Niña ($N = 353$) events in CAM5. Top row: polar stereographic sea level pressure (SLP) anomaly composites for El Niño (left column) and La Niña (right column) events. Middle row: North Atlantic surface wind stress ($\vec{\tau}$; vectors) and turbulent heat flux anomaly composites. Bottom row: North Atlantic mixed-layer depth anomaly composites. Statistical significance at the 95% level in the top and bottom rows is indicated by the hatching. In the middle row, only grid points that are statistically significant at the 95% level are either shaded or display a vector. Heat fluxes are positive into the ocean.

see the characteristic dipole SLP anomaly pattern of the NAO. In a composite mean sense, a negative NAO pattern (positive SLP anomalies in the subpolar North Atlantic and negative SLP anomalies in the subtropical North Atlantic (Hurrell *et al* 2013)) accompanies El Niño events and a positive NAO pattern accompanies La Niña events.

Although many GCMs and Earth System Models (ESMs) have biases in their representation of ENSO (Karamperidou *et al* 2017, Feng *et al* 2020), we note that the ENSO teleconnections in CAM5 are reasonably well-represented in the North Atlantic region

with a slight underestimation of the associated NAO pattern (Deser *et al* 2017). We find a similar connection between ENSO and the NAO in WACCM4 (see figure S1. Note that the main body of the paper shows plots for CAM5, while complimentary plots for WACCM4 are included in the supplementary material (available online at stacks.iop.org/ERL/16/084038/mmedia)).

These atmospheric NAO anomalies are associated with characteristic patterns of air-sea coupling. Figures 1(c) and (d) show El Niño and La Niña composites of wintertime surface wind stress ($\vec{\tau}$; vectors)

and turbulent (sensible and latent) heat flux anomalies in the North Atlantic region. The anomaly patterns are typical of those associated with the NAO (Frankignoul 1985, Cayan 1992, Deser and Timlin 1997, Wen *et al* 2005, Visbeck *et al* 2013). For El Niño (figure 1(c)), we find anomalously westward surface wind stress north of 40° N and anomalously eastward surface wind stress south of 40° N. This is associated with a reduced turbulent heat flux from the ocean to the atmosphere north of 40° N, i.e. anomalously positive turbulent heat flux into the ocean. We see slightly weaker and oppositely signed patterns for La Niña (figure 1(d)). The SST anomalies (figure S2) that accompany these wind stress and turbulent heat flux anomalies exhibit the characteristic tripolar pattern associated with the NAO; for El Niño, we find positive SST anomalies in the subpolar and tropical regions and negative SST anomalies in the subtropics. Note that the SST anomalies along the coast of Labrador are associated, in part, with negative and positive sea ice concentration anomalies for the El Niño and La Niña composites, respectively (not shown) (Strong *et al* 2009).

Given the significant impact of ENSO via the NAO on the air-sea exchange of heat and momentum over the North Atlantic, we now explore the possibility that ENSO may actually be able to impact the AMOC (via the NAO). Previous studies have examined both the impact of ENSO and the NAO on the AMOC, but have focused on the annual mean AMOC and have found little evidence of a significant effect on interannual timescales (Mignot and Frankignoul 2005, Delworth and Zeng 2016). Here we restrict our analysis to the wintertime AMOC and show that there is indeed a significant effect of ENSO on the wintertime AMOC.

We begin by examining the effect of ENSO on the mixed-layer depth, using the mixed-layer depth definition based on the buoyancy gradient approach described in Large *et al* (1997). Figures 1(e) and (f) show El Niño and La Niña composites of wintertime mixed-layer depth anomalies in the North Atlantic region. We clearly see significant anomalies in the Labrador Sea region, the primary region of convection and deep water formation in the North Atlantic. During El Niño events, when the mixed layer is heated via turbulent heat flux anomalies and momentum is extracted from the mixed-layer via surface wind stress anomalies, we find that the mixed layer shoals by approximately 50–100 m in the Labrador Sea region. We see the opposite during La Niña events, a deepening of the mixed layer by approximately 25–50 m in the Labrador Sea region. The question remains whether the influence of these wind stress, heat flux and mixed-layer depth anomalies is restricted to the surface ocean or is associated with large-scale changes in the AMOC itself.
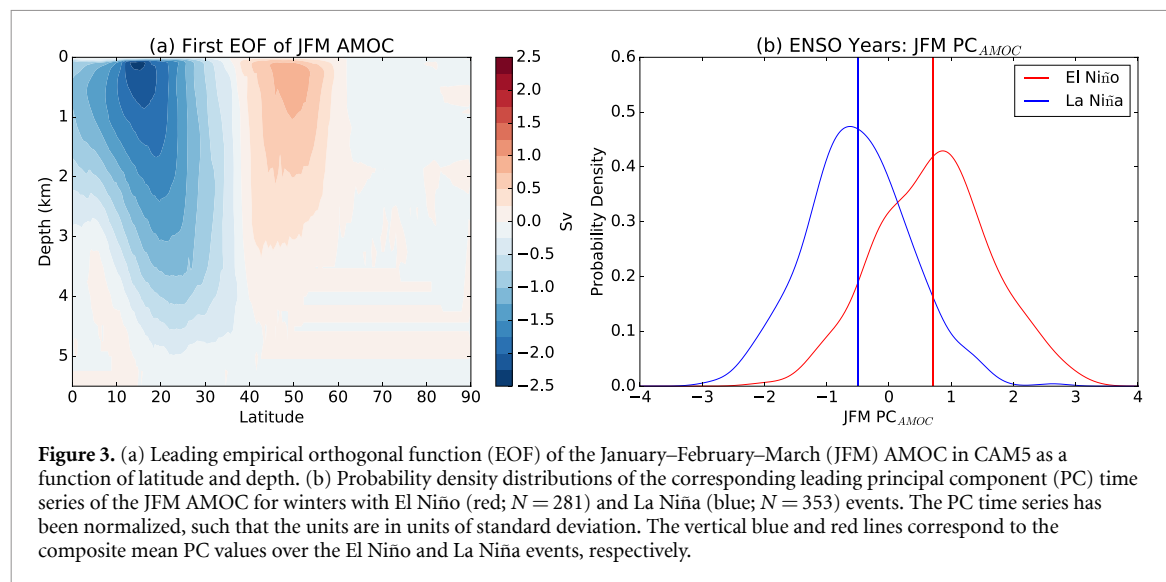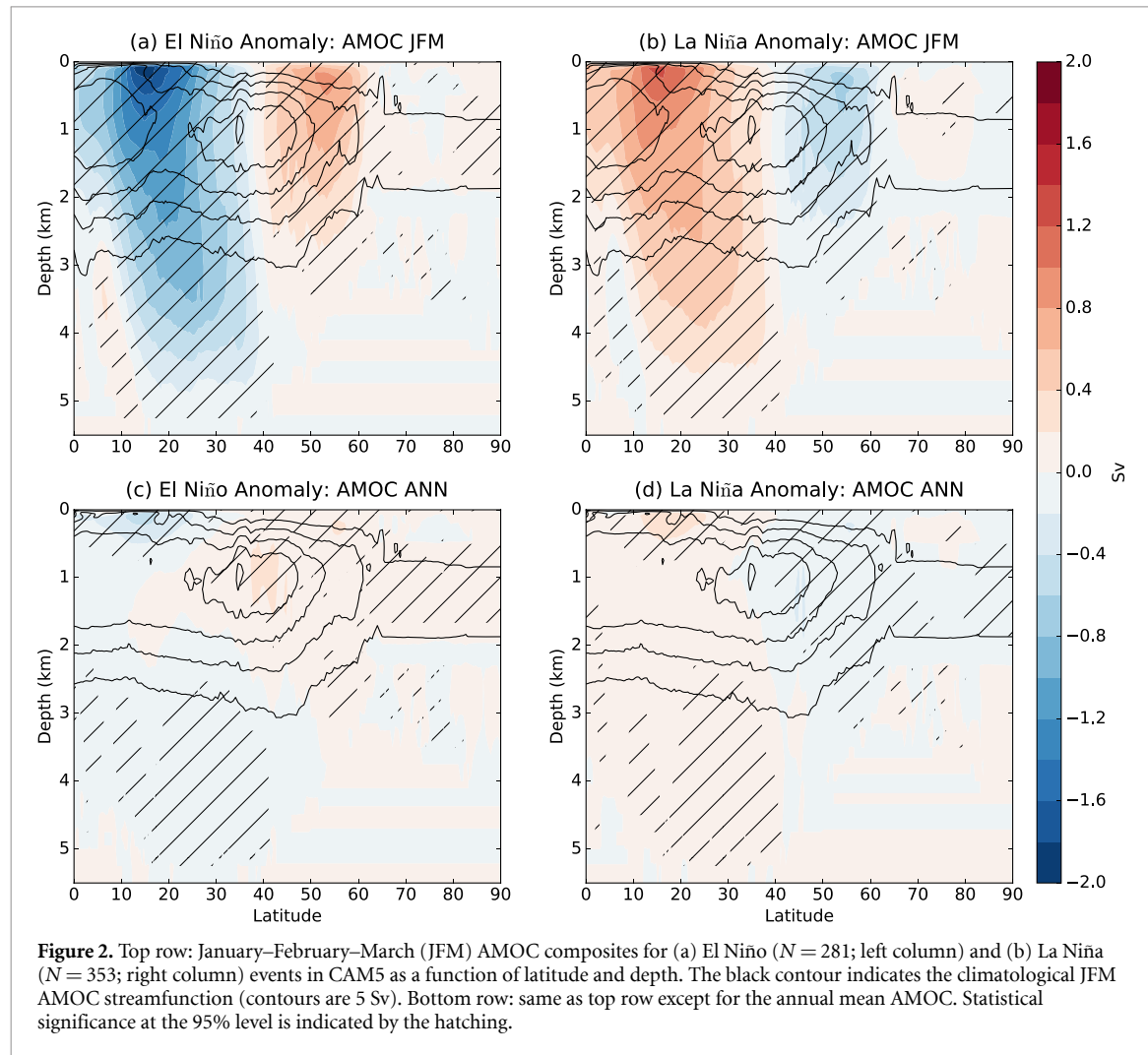
To address this question, we now present our key finding. Figures 2(a) and (b) show El Niño and La Niña composites of wintertime AMOC anomalies (see also figure S3 for WACCM4). We find significant anomalies in the large-scale circulation that extend well-below the Ekman layer. Specifically, during El Niño events the AMOC significantly weakens to the south of approximately 40° N and significantly strengthens north of 40° N. The southern anomalies extend throughout the depth of the Atlantic Basin, while the northern anomalies are restricted to the upper 2–3 km. Slightly weaker and opposite-signed AMOC anomalies occur during La Niña events. The AMOC anomalies associated with ENSO approximately represent a shift about the climatological winter maximum streamline (see black contours in figure 2). The anomalies are largest at the surface and decay with depth.

Given that we are considering interannual wintertime anomalies rather than long-term averages, the vertical structure of the AMOC anomalies suggests a process of oceanic adjustment. Near the surface, we find wind-driven Ekman transport anomalies and at depth, corresponding compensating flow anomalies with a baroclinic structure (Tandon *et al* 2020). Notably, the AMOC anomalies at high-latitudes are opposite in sign to what might be expected if changes in Labrador Sea deep water formation were the dominant factor (figures 1(e) and (f)), demonstrating the key role of the wind stress anomalies. The opposing effects of deep water formation and wind forcing at high-latitudes may contribute to the weaker circulation of the northern cell compared to its southern counterpart.

As a point of comparison, we also show El Niño and La Niña composites of the *annual mean* AMOC in figures 2(c) and (d) (see also figure S3 for WACCM4). Very little of the winter ENSO signal is seen in the annual mean AMOC, highlighting that detection of an interannual link between ENSO and the AMOC will fail if only the annual mean AMOC is considered.

To assess the importance of this wintertime pattern of AMOC variability, we perform a PC analysis and extract the leading mode of wintertime AMOC variability in CAM5. The spatial pattern of the leading mode, i.e. the first empirical orthogonal function (EOF), (figures 3(a) and S4(a) for WACCM4) is strikingly similar to the pattern of the ENSO composite AMOC anomalies shown in figures 2(a) and (b) and reminiscent of the NAO-associated mode described in Elipot *et al* (2017). In CAM5, the first EOF accounts for more than half of the variance in the wintertime AMOC with 52% of the variance explained (the variance explained by the second and third EOFs are 12% and 9%, respectively). It is important to note that the nature of this EOF pattern is quite distinct from the leading EOF of the annual mean AMOC, which shows a basin-scale pattern (Danabasoglu *et al* 2012). Complementary statistics for WACCM4 are included in the supplementary material (text S1).

Figure 2. Top row: January–February–March (JFM) AMOC composites for (a) El Niño ($N = 281$; left column) and (b) La Niña ($N = 353$; right column) events in CAM5 as a function of latitude and depth. The black contour indicates the climatological JFM AMOC streamfunction (contours are 5 Sv). Bottom row: same as top row except for the annual mean AMOC. Statistical significance at the 95% level is indicated by the hatching.

Figure 3. (a) Leading empirical orthogonal function (EOF) of the January–February–March (JFM) AMOC in CAM5 as a function of latitude and depth. (b) Probability density distributions of the corresponding leading principal component (PC) time series of the JFM AMOC for winters with El Niño (red; $N = 281$) and La Niña (blue; $N = 353$) events. The PC time series has been normalized, such that the units are in units of standard deviation. The vertical blue and red lines correspond to the composite mean PC values over the El Niño and La Niña events, respectively.

The role of ENSO in contributing to this mode of variability can be illustrated by isolating years of the PC time series that correspond to El Niño and La Niña events. Figure 3(b) (figure S4(b) for WACCM4) shows the probability density distributions (PDFs) of these PC values (in units of standard deviation) for the El Niño (red) and La Niña (blue) winters. We clearly see that the PDFs are well-separated and this is confirmed by performing a Kologorov–Smirnov test, which indicates that the two distributions are significantly distinct.

We also find that the correlation between the leading PC time series of the winter AMOC and the winter ENSO index is quite high and statistically significant at the 95% level ($R^2 = 25.6\%$), while the correlation between the leading PC time series of the annual mean AMOC and the winter ENSO index is very low, but also statistically significant given the large sample size ($R^2 = 3.5\%$). This helps to explain why studies of the annual mean AMOC may have overlooked this significant link between ENSO and the AMOC in winter. Furthermore, we find that the correlation between the leading PC time series of the winter AMOC and the winter NAO index is somewhat lower, but statistically significant ($R^2 = 17.5\%$) than for the winter ENSO index. Thus, we find that the winter AMOC appears to be more strongly influenced by the ENSO-NAO teleconnection rather than the NAO itself. Given that the NAO is not entirely independent of ENSO, this may be related to certain characteristics of the NAO, such as the persistence of the NAO in the presence of ENSO due to local atmosphere-ocean feedbacks (Alexander and Scott 2008, Hu *et al* 2011). This finding requires further study; however, we do not have sufficient daily model output to examine this at this time.

4. Conclusions

Using long, fully-coupled control integrations of CAM5 and WACCM4, we have here shown that the wintertime AMOC exhibits a distinct mode of variability that appears to be strongly influenced by ENSO via the NAO. The dipole pattern of variability about the wintertime AMOC maximum resembles an Ekman-induced baroclinic adjustment (Elipot *et al* 2017, Tandon *et al* 2020).

Although these findings are model-based and restricted to only two GCMs, they support the growing observational evidence for substantial high-frequency AMOC variability. This variability that has been primarily attributed to local wind forcing, but its distinct seasonal nature and connection to remote sources of variability, such as ENSO, have been largely overlooked in previous studies (e.g. Mignot and Frankignoul 2005, Balan Sarojini *et al* 2011, Delworth and Zeng 2016).

Further work is required to establish the climate implications of such a mode of wintertime AMOC variability (Delworth *et al* 2016). However, our finding will help with the interpretation of the ongoing AMOC measurements being collected by trans-Atlantic arrays (Frajka-Williams *et al* 2019). Distinguishing anthropogenic trends from internal variability is a complex, yet very important, task when analyzing in-situ observations. Work such as this highlight that there may be significant sources of internal variability that are yet to be fully explored.

ORCID iDs

K L Smith ⬤ https://orcid.org/0000-0002-4652-6310
L M Polvani ⬤ https://orcid.org/0000-0003-4775-8110

References

Alexander M A and Scott J D 2008 The role of Ekman ocean heat transport in the northern hemisphere response to ENSO *J. Clim.* **21** 5688–707

Balan Sarojini B *et al* 2011 High frequency variability of the Atlantic Meridional Overturning Circulation *Ocean Sci.* **7** 471–86

Buckley M W and Marshall J 2016 Observations, inferences and mechanisms of the Atlantic meridional overturning circulation: a review *Rev. Geophys.* **54** 5–63

Cayan D R 1992 Latent and sensible heat flux anomalies over the northern oceans: driving the sea surface temperature *J. Phys. Oceanogr.* **22** 859–81

Cunningham S A *et al* 2007 Temporal variability of the Atlantic meridional overturning circulation at 26.5° N *Science* **317** 935–9

Danabasoglu G 2008 On multidecadal variability of the Atlantic meridional overturning circulation in the community climate system model version 3 *J. Clim.* **21** 5524–44

Danabasoglu G, Yeager S G, Kwon Y-O, Tribbia J J, Phillips A S and Hurrell J W 2012 Variability of the Atlantic meridional overturning circulation in CCSM4 *J. Clim.* **25** 5153–72

Delworth T L and Zeng F 2016 The impact of the north Atlantic oscillation on climate through its influence on the Atlantic meridional overturning circulation *J. Clim.* **29** 941–62

Delworth T L, Zeng F, Vecchi G A, Yang X, Zhang L and Zhang R 2016 The north Atlantic oscillation as a driver of rapid climate change in the northern hemisphere *Nat. Geosci.* **9** 509–13

Delworth T L, Zeng F, Zhang L, Zhang R, Vecchi G and Yang X 2017 The central role of ocean dynamics in connecting the north Atlantic oscillation to the extratropical component of the Atlantic multidecadal oscillation *J. Clim.* **30** 3789–805

Deser C, Simspon I R, MacKinnon K A and Phillips A S 2017 The northern hemisphere extratropical atmospheric circulation

response to ENSO: how well do we know it and how do we evaluate models accordingly? *J. Clim.* **30** 5059–82

Deser C and Timlin M S 1997 Atmosphere–ocean interaction on weekly timescales in the north Atlantic and pacific *J. Clim.* **10** 393–408

Elipot S, Frajka-Williams E, Hughes C W, Olhede S and Lankhorst M 2017 Observed basin-scale response of the north Atlantic meridional overturning circulation to wind stress forcing *J. Clim.* **30** 2029–54

Feng J, Lian T, Ying J, Li J and Li G 2020 Do CMIP5 models show El Niño diversity? *J. Clim.* **33** 1619–41

Frajka-Williams E *et al* 2019 Atlantic meridional overturning circulation: observed transport and variability *Front. Mar. Sci.* **6** 260

Frankignoul C 1985 Sea surface temperature anomalies, planetary waves and air-sea feedback in the middle latitudes *Rev. Geophys.* **23** 357–90

Gent P R *et al* 2011 The community climate system model version 4 *J. Clim.* **24** 4973–91

Hu Z-Z, Kumar A, Huang B, Xue Y, Wang W and Jha B 2011 Persistent atmospheric and oceanic anomalies in the north Atlantic from summer 2009 to summer 2010 *J. Clim.* **24** 5812–30

Hurrell J W, Holland M and Gent P R 2013 The community earth system model: a framework for collaborative research *Bull. Am. Meteorol. Soc.* **94** 1339–60

Hurrell J W, Kushnir Y, Ottersen G and Visbeck M 2013 *An Overview of the North Atlantic Oscillation* (Washington, DC: American Geophysical Union) pp 1–35

Kanzow T *et al* 2010 Seasonal variability of the Atlantic meridional overturning circulation at 26.5° N *J. Clim.* **23** 5678–98

Karamperidou C, Jin F-F and Conroy J L 2017 The importance of ENSO nonlinearities in tropical pacific response to external forcing *Clim. Dyn.* **49** 2695–704

Kay J E *et al* 2015 The community earth system model (CESM) large ensemble project: a community resource for studying climate change in the presence of internal climate variability *Bull. Am. Meteorol. Soc.* **96** 1333–49

Knight J R, Allan R J, Folland C K, Vellinga M and Mann M E 2005 A signature of persistent natural thermohaline circulation cycles in observed climate *Geophys. Res. Lett.* **32** 2–5

Large W G, Danabasoglu G, Doney S C and McWilliams J C 1997 Sensitivity to surface forcing and boundary layer mixing in a global ocean model: annual-mean climatology *J. Clim.* **27** 2418–47

Marsh D R, Mills M J, Kinnison D E, Lamarque J-F, Calvo N and Polvani L M 2013 Climate change from 1850 to 2005 simulated in CESM1(WACCM) *J. Clim.* **26** 7372–91

Mezzina B, Garcia-Serrano J, Blade I and Kucharski F 2020 Dynamics of the ENSO teleconnection and NAO variability in the north Atlantic–European late winter *J. Clim.* **33** 907–23

Mignot J and Frankignoul C 2005 The variability of the Atlantic meridional overturning circulation, the north Atlantic oscillation and the El Niño-southern oscillation in the Bergen climate model *J. Clim.* **18** 2361–75

Neale R B *et al* 2010 Description of the NCAR community atmosphere model (CAM 5.0) *Technical Report* NCAR Technical Note TN-486

Polvani L M, Sun L, Butler A H, Richter J H and Deser C 2017 Distinguishing stratospheric sudden warmings from ENSO as key drivers of wintertime climate variability over the North Atlantic and Eurasia *J. Clim.* **30** 1959–69

Roberts C D *et al* 2013 Atmosphere drives recent interannual variability of the Atlantic meridional overturning circulation at 26.5° N *Geophys. Res. Lett.* **40** 5164–70

Rodríguez-fonseca B, Suárez-moreno R, Ayarzagüena B, López-parages J, Gómara I, Villamayor J, Mohino E, Losada T and Castaño-tierno A 2016 A review of ENSO influence on the North Atlantic. A non-stationary signal *Atmosphere* **7** 1–19

Smeed D A *et al* 2014 Observed decline of the Atlantic meridional overturning circulation *Ocean Sci.* **10** 29–38

Smith K, Polvani L and Tremblay L 2018 The impact of stratospheric circulation extremes on minimum arctic sea ice extent *J. Clim.* **31** 7169–83

Strong C, Magnusdottir G and Stern H 2009 Observed feedback between winter sea ice and the north Atlantic oscillation *J. Clim.* **22** 6021–32

Tandon N F, Saenko O A, Cane M A and Kushner P J 2020 Interannual variability of the global meridional overturning circulation dominated by pacific variability *J. Phys. Oceanogr.* **50** 559–74

Visbeck M, Chassignet E P, Curry R G, Delworth T L, Dickson R R and Krahmann G 2013 *The Ocean's Response to North Atlantic Oscillation Variability* (Washington, DC: American Geophysical Union) pp 113–45

Wen N, Liu Z, Liu Q and Frankignoul C 2005 Observations of SST, heat flux and North Atlantic ocean-atmosphere interaction *Geophys. Res. Lett.* **32** 2–5

Zhang R, Delworth T L and Held I M 2007 Can the Atlantic ocean drive the observed multidecadal variability in northern hemisphere mean temperature? *Geophys. Res. Lett.* **34** 1–6

Zhao J and Johns W 2014 Wind-forced interannual variability of the Atlantic meridional overturning circulation at 26.5° N *J. Geophys. Res.: Oceans* **119** 2403–19